Journal Name

Dynamic Article Links ►

Cite this: DOI: 10.1039/c0xx00000x

www.rsc.org/xxxxxx

ARTICLE TYPE

Novel lithium-laded porous aromatic framework for efficient CO_2 and H_2 uptake

Heping Ma,[a] Hao Ren,[a] Xiaoqin Zou,[a] Fuxing Sun,[a] Zhuojun Yan,[a] Kun Cai,[a] Dayang Wang [b] and Guangshan Zhu*[a,c]

Received (in XXX, XXX) Xth XXXXXXXXX 200X, Accepted Xth XXXXXXXXX 200X
DOI: 10.1039/b000000x

Novel porous aromatic frameworks, PAF-18-OH and its lithiated derivative PAF-18-OLi, have been successfully synthesized. In particular, PAF-18-OLi displays significant enhancements of H_2 and CO_2 adsorption capacity, especially for the CO_2 uptake (14.4 wt%). More valuably, the stable PAF-18-OLi material exhibits high CO_2/N_2 selectivity, as high as 129 in the case of CO_2 capture from simulated post-combustion flue gas mixtures (85% N_2 and 15% CO_2). Furthermore, the PAF-18-OLi has shown an improved H_2 storage capacity after lithiation.

Introduction

The environmental degeneration and adverse climate change are currently two of the challenges mostly affecting our daily life.[1] The increasing utilization of world's fast diminishing fossil fuels is the major source of environmental pollution.[2] The emission of CO_2 is considered as the most significant contribution to the global warming among all of the Earth's radiative-forcing components.[3] To solve these two pressing environmental issues, it requires the development of new technologies for capture and sequestration of CO_2 and efficiently harness a range of renewable energy sources and carriers such as H_2.[4] Porous materials, such as activated carbon,[5] zeolites,[6] and metal–organic frameworks (MOFs),[7] have demonstrated a promising prospect in applications for H_2 storage and CO_2 capture owing to their high specific surface areas and low energy consumption for regeneration. Recently, a new family of porous materials, porous organic frameworks (POFs), composed of light elements (C, H, O, N, B, etc) via covalent bonds, have attracted a great deal of attention thanks to their high surface areas, high stability and controllable skeletons.[8-13] Current investigations have demonstrated that POFs are promising materials for H_2 storage and CO_2 capture.[14]

Up to date, H_2 storage in porous materials are usually implemented under either high pressure or very low temperature conditions, which are not easily adapted in commercial and realistic applications.[2a] Traditional CO_2 capture is based on the chemical absorption of CO_2 using the aqueous solutions of amines,[15] and a substantially large amount of energy are required for the activity regeneration of the amines. Although the use of porous materials for physical adsorption of CO_2 is fairly energy-effective, the considerable amount of N_2 are co-adsorbed in the porous materials, resulting in low CO_2/N_2 selectivity.[16] To enhance H_2 or CO_2 uptake and especially improve the CO_2/N_2 adsorption selectivity, porous materials should possess strong interaction with H_2 or CO_2. Several strategies in literatures have been developed to enhance the interactions between porous materials and gas molecules via the control of the pore size, incorporation of polar functional groups or introduction of open metal sites into the porous networks.[17] For instance, doping atomically dispersed alkali metal cations, for example Li^+ ions into MOFs and POFs is expected to increase H_2 and CO_2 storage capacities.[18,19a] However, Li^+-doped MOFs or POFs have limited success in H_2 storage and CO_2 capture due to the instability of Li^+ ions or the modified porous structures.[19] Herein we synthesized new porous aromatic frameworks (PAFs) with permanent porosity and functionalized OH groups, referred as PAF-18-OH. The OH groups of PAF-18-OH have been further transformed into the lithium alkoxy groups, resulted in lithium-laded PAF, referred as PAF-18-OLi (Scheme 1).

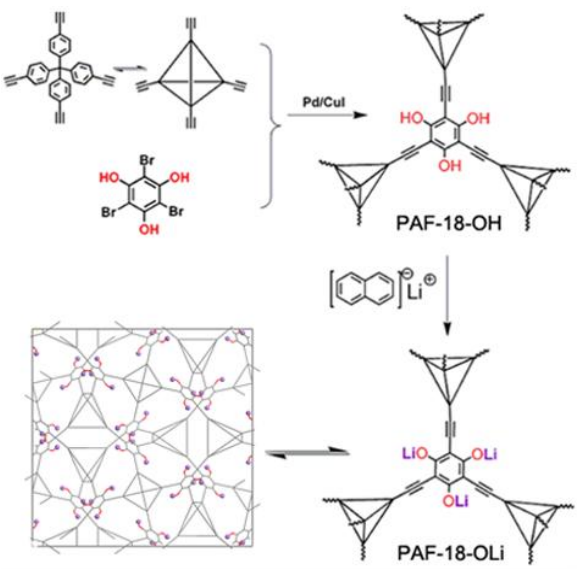

Scheme 1 Schematic depict for the synthesis of PAF-18-OH and PAF-18-OLi.

PAF-18-OLi has exhibited a significantly increased uptake of CO_2 with high CO_2/N_2 selectivity as large as 129 at 273 K. Furthermore, the PAF-18-OLi has shown an enhanced H_2 storage capacity.

Experimental section

Chemicals:

All chemicals were purchased from Aldrich, Alfa-Aesar, and Aladdin-reagent, and used as received unless it was noted. *N*,*N*-Dimethylformamide (DMF) and triethylamine (Et_3N) were dehydrated with CaH_2. Tetrahydrofuran (THF) was distilled in the presence of sodium benzophenone ketyl under N_2 condition. Tetrakis(4-ethynylphenyl)methane[20a] and 2,4,6-Tribromo-benzene-1,3,5-triol[20b] were prepared according to the previously reported method.

Synthesis of PAF-18-OH:

Tetrakis(4-ethynylphenyl)methane (125 mg, 1.5 mmol), 2,4,6-tribromo-benzene-1,3,5-triol (116 mg, 1.5 mmol), tetrakis(triphenphosphine)palladium (30 mg), and copper iodide (8 mg) were dissolved in the mixture of DMF (5 mL) and Et_3N (5 mL) in a 50 mL two-necked flask, After degassing via three freeze-pump-thaw cycles, the mixture was stirred at 85 ^oC for 36 h under N_2. After cooling down to room temperature, the resulting PAF-18-OH was collected by filtration, followed by consecutive washing by Soxhlet extraction for 48 h with THF, methanol to remove the unreacted monomers or catalysts. After drying at 90 ^oC in vacuum overnight, PAF-18-OH was obtained in the form of brown powder (150 mg, 90% yield).

Synthesis of PAF-18-OLi:

Synthesis of PAF-18-OLi was performed in an argon atmosphere glove box. Lithium-naphthalenide ($Li^+C_{10}H_8^-$) was synthesized by adding small pieces of clean lithium (3 mg, stored in glove box) into 100 mL naphthalene solution in THF (0.1 M), followed by 4 h vigorous stirring. After reaction, the solution became dark green; a given volume of this solution was taken out by a volumetric syringe and mixed with the dried powders of PAF-18-OH with a given mass (see supporting information). After stirring overnight to ensure the complete reaction of $Li^+C_{10}H_8^-$ with PAF-18-OH, the powder of PAF-18-OLi was filtrated and washed with THF for several times to remove naphthalene and then dried under vacuum at 120 ^oC for 12 h.

Characterizations:

FTIR spectra were obtained using an IFS 66V/S Fourier transform infrared spectrometer. Thermogravimetric analysis (TG) was implemented using a Netzch Sta 449c thermal analyzer system at a heat rate of 10 °C/min under air. Scanning electron microscopy (SEM) imaging was performed on JEOS JSM 6700. Transmission electron microscopy (TEM) imaging was carried out on JEOL JEM 3010 with an acceleration voltage of 300 kV. X-ray photoelectron spectroscopy (XPS, ESCALAB 250, Thermo Scientific) was performed by using a monochromatized Al Kα (1486.6 eV) X-ray source. ^7Li MAS NMR spectra were recorded on a Bruker AVANCE III 400 WB spectrometer. Powder X-ray diffraction (PXRD) was carried out by a Riguku D/MAX2550 diffractometer using CuKα radiation, 40 kV, 200 mA with scanning rate of 3 °/min (2θ). The lithium content in PAF-18-OLi was determined by inductively coupled plasma (ICP) spectroscopy (Perkin-Elmer ICP-OES Optima 3300DV). Before analysis, ~15 mg sample was digested in 3:1 HCl/HNO_3 (10 mL) and transferred to 50 mL volumetric flask with distilled water.

Low-pressure gas adsorption measurements:

The gas adsorption/desorption isotherms were measured on a Quantachrome Autosorb iQ2 analyzer. N_2 adsorption/desorption measurements were carried out at 77 K, 273 K, and 298 K; H_2 adsorption/desorption isotherms recorded at 77 K and 87 K; and CO_2 adsorption/desorption isotherms collected at 273 K and 298 K, respectively. Ultra-high-purity grade (99.99%) N_2, H_2, and CO_2 gases were used for all adsorption measurements. Liquid nitrogen and liquid argon bathes were utilized to control the temperature at 77 K and 87 K, respectively. Ice-water bath and water bathes equipped with a temperature sensor were used to control the temperature at 273 K and 298 K.

Results and discussion

Description of PAF-18-OH and PAF-18-OLi:

PAF-18-OH was synthesized via palladium-catalyzed Sonogashira-Hagihara cross-coupling reaction of tetrahedral tetrakis(4-ethynylphenyl)methane (TEPM) and triangle 2,4,6-Tribromo-benzene-1,3,5-triol (TBBT).[21] The resulted product is characterized by PXRD and the XRD pattern shows that the product is in amorphous phase (Fig. S1). The ^{13}C CP-MAS NMR spectrum confirms the successful synthesis of PAF-18-OH with the characteristic peaks from the joint monomers (Fig. S2). The FT-IR spectra of as-prepared PAF-18-OH clearly indicate the presence of OH groups (Fig. S3a). The thermogravimetric analysis (TG) shows the decomposition of PAF-18-OH is started at the temperature of 350 ^oC under air (Fig. S4), suggesting this material possesses an excellent thermal stability. The PAF-18-OH is insoluble in common organic solvents, such as THF, acetone, ethanol, DMF, and DMSO, indicating a highly chemical stability.

After reaction with lithium naphthalenide ($Li^+C_{10}H_8^-$ in THF),[22] the protons of PAF-18-OH are replaced by Li ions, yielding PAF-18-OLi. The complete lithiation of PAF-18-OH has been confirmed by the disappearance of the OH stretching vibration band centered at 3432 cm^{-1} in the FT-IR spectrum of PAF-18-OLi (Fig. S3b). The Li content of PAF-18-OLi could readily tuned by altering the molar ratio of $Li^+C_{10}H_8^-$ to the OH groups of PAF-18-OH. In our work, the complete lithation yields a maximum Li content of 4.2 wt% in the resulting PAF-18-OLi, very close to the theoretical value, 4.5 wt%. The high-resolution XPS (Fig. S5) and ^7Li MAS NMR spectroscopy (Fig. S6) analyses of PAF-18-OLi indicate that Li is present at the ionic state in a high-purity PAF material.[23]

Further, the morphologies of PAF-18-OH and its derivative PAF-18-OLi are monitored by scanning electron microscopy (SEM). SEM images show both PAF-18-OH and PAF-18-OLi are aggregates of microgel particles with a size of 100 nm (Fig. 1a and 1b). The appearance of PAF-18-OLi is similar to PAF-18-OH, indicating the structure of PAF-18-OLi is preserved after lithiation. In addition, the microstructure is studied by transmission electron microscopy (TEM). The TEM images of PAF-18-OH and PAF-18-OLi are displayed in Fig. 1c and d. As can be seen, the worm-like porous texture is observed in both materials.

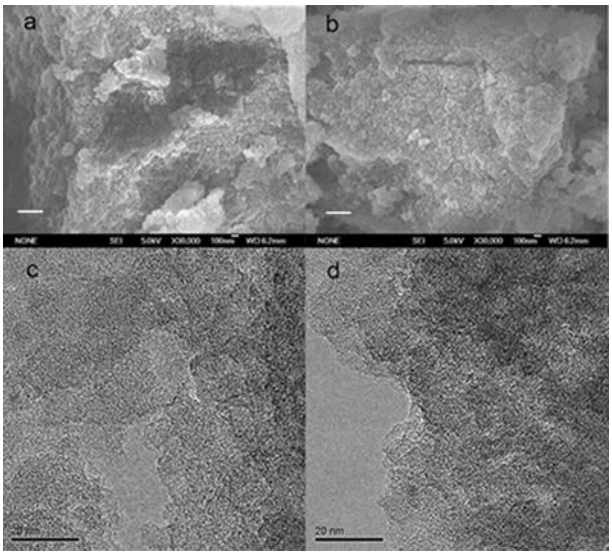

Fig. 1 SEM images of PAF-18-OH (a) PAF-18-OLi (b), scale bars: 300 nm. TEM images of PAF-18-OH (c) PAF-18-OLi (d), scale bars: 20 nm.

Porosity of PAF-18-OH and PAF-18-OLi:

The porosity of PAF-18-OH and PAF-18-OLi is probed with physical nitrogen sorption at 77 K. A sharp increase in gas uptake is observed at low pressure in the nitrogen adsorption-desorption isotherms of PAF-18-OH and PAF-18-OLi, which further confirms an existence of the micropores in both PAFs; a distinct adsorption–desorption hysteresis at high relative pressure sheds light on the presence of some mesopores, which is a common character for many porous organic frameworks (Fig. 2a).[24,18c]

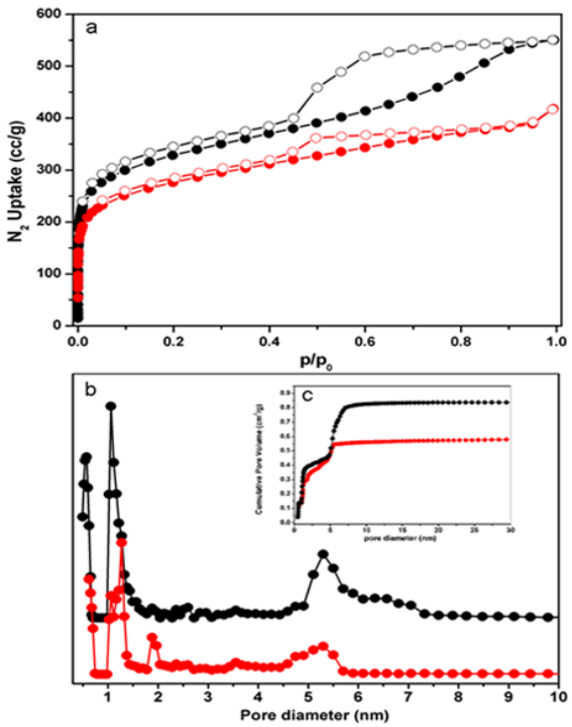

Fig. 2 (a) N_2 adsorption (solid circles) and desorption (open circles) isotherms of PAF-18-OH (black symbols) and PAF-18-OLi (red symbols) at 77K; (b) the pore size distribution of PAF-18-OH (black circles) and PAF-18-OLi (red circles), (c) the corresponding cumulative pore volume distributions are shown in the inset.

The Brunauer-Emmett-Teller (BET) surface area of PAF-18-OH is measured as 1121 $m^2 g^{-1}$. As shown in Fig. 2a, the lithiation of PAF-18-OH causes a small reduction in the BET surface area. The BET surface areas of PAF-18-OLi are decreasing with an increase of the lithium content. Typically, the surface area of 981 $m^2 g^{-1}$ is obtained after the complete lithation (Li content is 4.2 wt%) (Table S1). The pore size distributions of PAF-18-OH and PAF-18-OLi have been calculated based on nonlocal density functional theory. As shown in Fig. 2b, the transformation of the OH groups into the lithium alkoxy groups gives negligible change of the pore size distribution within the PAF-18 materials (Table 1). The little change in pore width is interpreted by the very close radius of ionic lithium and the hydrogen atom. But an increase of the density after lithiation causes noticeable decrease in the pore volume (Fig. 2c), which is the same phenomenon observed in the small reduction of the surface areas of the PAFs. The calculated pore volumes for PAF-18-OH and PAF-18-OLi are 0.82 and 0.57 $cm^3 g^{-1}$, respectively. Also, PAF-18-OLi exhibits a micropore volume of 0.34 $cm^3 g^{-1}$, which is a bit less than that of PAF-18-OH (0.4 $cm^3 g^{-1}$).

The CO_2 adsorption for PAF-18-OH and PAF-18-OLi:

Given the particular polarity of PAF-18-OH and PAF-18-OLi for effective adsorption of CO_2,[17] the -OLi in PAFs may provide strong polar open coordination sites, which could result in stronger interactions with CO_2 molecules. The CO_2 adsorption is studied on both PAF-18-OH and PAF-18-OLi samples (Fig. 3).

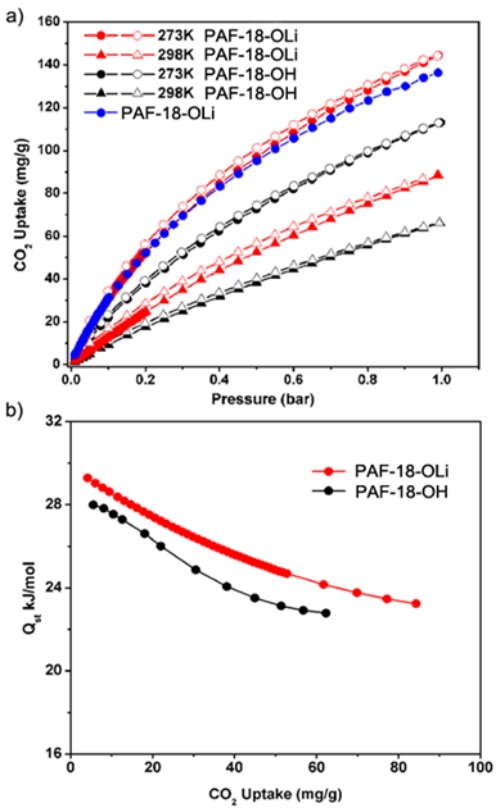

Fig. 3 (a) CO_2 adsorption (solid symbols) and desorption (open symbols) isotherms of PAF-18-OH and PAF-18-OLi at 273 K and 298 K. CO_2 adsorption of PAF-18-OLi obtained after 10 days exposure in wet air (blue circles) at 273K. (b) Plots of the isosteric heat of adsorption (Q_{st}) for CO_2 of PAF-18-OH and PAF-18-OLi versus CO_2 uptake.

Table 1 The properties of porosity, gas uptake and isosteric heat of adsorption of PAF-18-OH and PAF-18-OLi.

Materials	BET ($m^2 g^{-1}$)	DFT pore diameter (nm)	Total pore volume ($cm^3 g^{-1}$)	Micropore volume ($cm^3 g^{-1}$)	CO_2 uptake 273K (wt%)	Q_{st} for CO_2 (kJ mol^{-1})	H_2 uptake 77K (wt%)	Q_{st} for H_2 (kJ mol^{-1})
PAF-18-OH	1121	1.33	0.82	0.4	11	28	1.35	7.4
PAF-18-OLi	981	1.32	0.57	0.34	14.4	29.5	1.65	7.6

Fig. 3a shows that the CO_2 uptake of PAF-18-OH is about 110 mg g^{-1} at 273 K and 66 mg g^{-1} at 298 K at 1 bar, respectively. The PAF-18-OLi with 4.2 wt % Li shows a maximum CO_2 uptake; 144 mg g^{-1} at 273 K and 89 mg g^{-1} at 298 K at 1 bar, respectively, which are comparable to the best CO_2 adsorption performances of lithiatied MOFs and POFs reported in the open literatures.[25] Additionally, in the case of PAF-18-OLi, the CO_2 uptake is increasing with more Li contents introduced into the PAF structure (Fig. S7a). When the Li content is larger than 4.2 wt%, the CO_2 uptake decreases distinctly. Excess lithium would aggregate on the skeleton surface, which poses a negative contribution to CO_2 uptake.

The affinity of guest molecules to host materials is usually evaluated by the isosteric heat of adsorption (Q_{st}).[26] Fig. 3b shows that PAF-18-OLi has a larger Q_{st} than that of PAF-18-OH; the Q_{st} value of PAF-18-OLi is slowly reduced from 29.5 kJ mol^{-1} to 23.5 kJ mol^{-1} as the CO_2 uptake reaches the maximum while the Q_{st} of PAF-18-OH from 28 kJ mol^{-1} to 23 kJ mol^{-1} (details of Q_{st} calculation in supporting information). Since the lithiation causes reduction in the surface area and pore volume, the enhanced CO_2 uptake (Fig. 3a) could be assigned to the presence of the Li ions in the PAF-18-OLi framework. It is usually envisioned that the Li ions in PAF-18-OLi create a high electric field on the framework surface, which leads to a high binding force with quadrupolar CO_2 molecules.[27] Due to the high activity of Li ions, Li doped MOFs and POFs are usually unstable under the wet condition.[19b-c, e] To verify their stability under wet condition, PAF-18-OLi samples were exposed to wet air (the average relative humidity is about 65%) for 10 days. This treatment causes little reduction in the CO_2 uptake of the PAF-18-OLi, as shown in Fig. 3a. This promises a great potential for future application of PAF-18-OLi in rigorous conditions, such as wet and oxygen.

The CO_2 /N_2 selectivities of PAF-18-OH and PAF-18-OLi:

Carbon dioxide capture or storage from the flue gas (> 70% N_2 content) is critical to reduce global greenhouse effect.[4] On the other hand, CO_2 is a useful chemical raw resource in industry. From the environment and energy perspective views, it requires adsorbents with large CO_2 adsorption capacity but with low N_2 adsorption ability in the range of low pressure and at ambient temperature. The adsorption isotherms of PAF-18-OH and PAF-18-OLi for CO_2 are investigated at different temperature of 273 K and 298 K, the results are shown in Fig. 4. It is found that both PAF-18-OH and PAF-18-OLi exhibit a pronounced CO_2 uptake and a fairly low N_2 adsorption at pressure of < 1 bar. The different adsorption ability towards CO_2 and N_2 provides a basis on the selective capture of CO_2 from gas mixture streams. We have employed the ideal adsorption solution theory (IAST) to assess the merit of lithiation for CO_2/N_2 separation, the method of which has been documented to accurately predict binary gas mixture adsorption in many porous materials.[28]

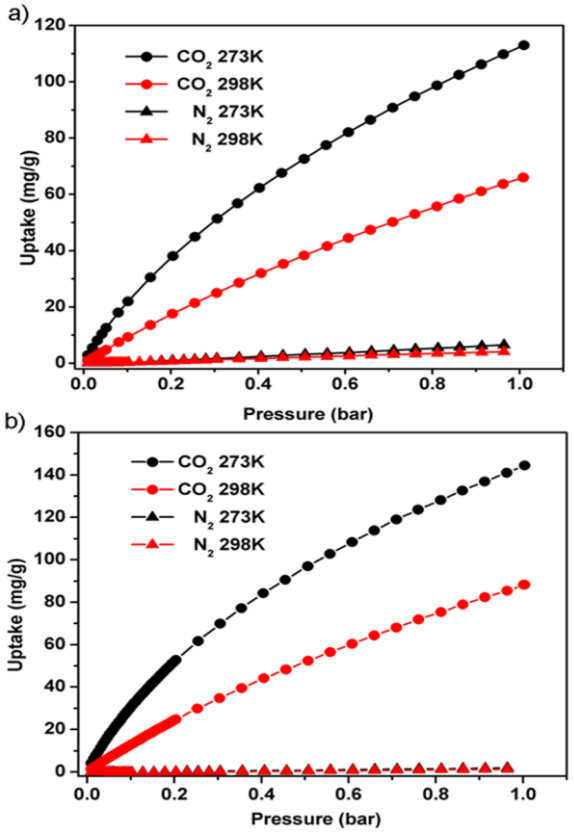

Fig. 4 The adsorption isotherms of CO_2 and N_2 at 273K and at 298K for PAF-18-OH (a) and PAF-18-OLi (b).

Dual-site Langmuir-Freundlich equation is used to fit the experimental single component adsorption isotherm. The selectivities of PAF-18-OH and PAF-18-OLi for CO_2 over N_2 in post-combustion flue gas stream (typically 15% CO_2 and 85% N_2) are shown in Fig. 5. The CO_2/N_2 selectivity is 34 for PAF-18-OH and 129 for PAF-18-OLi at 273 K, respectively. After temperature is elevated from 273 K to 298 K, the selectivities are correspondingly reduced to 16 for PAF-18-OH and 45 for PAF-18-OLi, respectively. The selectivity of PAF-18-OLi at 273 K is nearly four times higher than that of PAF-18-OH at the same conditions. The exceedingly high CO_2/N_2 selectivity of PAF-18-OLi could be attributed to the presence of the Li ions in the framework which drastically enhances the adsorption of polar CO_2 molecules, and the decrease in the BET surface area and pore volume limits N_2 uptakes.

Further, we have also studied the capture of CO_2 from low-pressure post-combustion flue gas mixtures with the CO_2 content of ~15 %. The CO_2 uptake is carried out at 0.15 bar and the N_2 adsorption at 0.85 bar, which is more relevant to practical application.

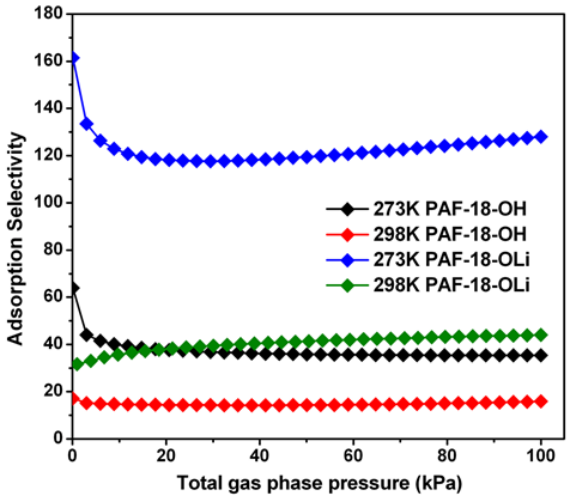

Fig. 5 IAST predicted 15 % CO_2 over 85 % N_2 adsorption selectivities for PAF-18-OH (black at 273 K and red at 298 K) and PAF-18-OLi (blue at 273 K and dark green at 298 K).

In this respect, the CO_2/N_2 selectivity in the flue gas is evaluated by the mass of CO_2 taken up at 0.15 bar divided by the mass of N_2 taken up at 0.85 bar. For example at 298 K (ambient temperature), the CO_2/N_2 selectivity of PAF-18-OH is estimated to be 4.3 whereas the value of 15.6 is calculated for PAF-18-OLi (Table 2). The tremendous increase in CO_2/N_2 selectivity for PAF-18-OLi can be due to high adsorption affinity of CO_2 onto available Li ions sites, simultaneously with the effect of a decline in the pore volume of PAF-18-OLi, which would greatly limit the nitrogen uptake in gas mixture if CO_2 is pre-adsorbed at ambient temperature and pressure (Fig. S8). To be mentioned, the selectivity of CO_2 over N_2 is increased in low temperature (273 K, see Table 2), which is in good agreement with the IAST predicted result. The enhanced CO_2/N_2 selectivity after lithiation provides a new approach to develop new type solid adsorbents for CO_2 capture and sequestration.

The H_2 adsorption for PAF-18-OH and PAF-18-OLi:

In the current work, we have also studied the possibility of PAF-18-OH and PAF-18-OLi for H_2 storage. Fig. 6a shows hydrogen adsorption isotherms for both PAF materials at 77 K and 87 K. Based on the isotherms, the H_2 uptake of PAF-18-OH is calculated to be 1.35 wt% at 77 K and 0.95 wt% at 87 K at 1 bar, respectively. After lithiation, the H_2 uptake has been significantly increased. The H_2 uptake of PAF-18-OLi increases with the Li content in PAF-18-OLi (Fig. S7b); while the Li content is exceeding 4.2 wt%, the H_2 uptake decreases (Fig. S7b).

Table 2 Summary of the CO_2/N_2 selectivity for PAF-18-OH and PAF-18-OLi.

Materials	273K $S^a_{(CO2/N2)}$ [1]	298K $S^a_{(CO2/N2)}$	273K $S^b_{(CO2/N2)}$ [2]	298K $S^b_{(CO2/N2)}$
PAF-18-OH	34	16	8.4	4.3
PAF-18-OLi	129	45	25	15.6

[1] $S^a_{(CO2/N2)}$ is calculated by IAST model from 85% N_2 and 15% CO_2, 1 atm.

[2] $S^b_{(CO2/N2)}$ is calculated by dividing the mass of CO_2 taken up at 0.15 bar by that of N_2 taken up at 0.85 bar.

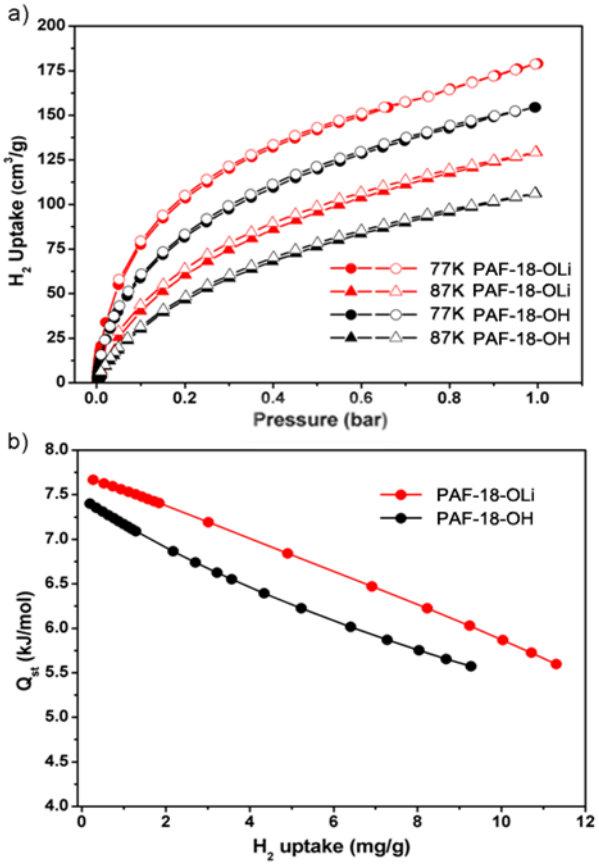

Fig. 6 (a) H_2 adsorption (solid symbols) and desorption (open symbols) isotherms of PAF-18-OH and PAF-18-OLi at 77 K and 87 K; (b) Plots of H_2 adsorption Q_{st} of PAF-18-OH and PAF-18-OLi versus the H_2 uptake.

PAF-18-OLi with the complete lithiation Li content of 4.2 wt% shows a maximum uptake of 1.65 wt% at 77 K and 1.17 wt% at 87 K at 1 bar, respectively. Additionally, the Q_{st} is calculated from the H_2 adsorption data at 77 K and 87 K using the virial method (details in supporting information).[26] Fig. 6b shows that the Q_{st} of PAF-18-OLi is higher than that of PAF-18-OH. This suggests that the Li ions in PAF-18-OLi promotes strong mutual interactions between hydrogen molecules and the PAF framework.

Conclusions

In conclusion, we have synthesized novel porous aromatic frameworks, PAF-18-OH and its lithiated derivative, PAF-18-OLi via Sonogashira-Hagihara cross-coupling reaction. The tunability of Li contents in PAF-18-OLi shows different capacities for CO_2 and H_2 adsorption. The complete lithiated PAF-18-OLi exhibits the highest CO_2 and H_2 adsorption ability, which is due to stronger interaction of gas molecules with lithium derivative PAF framework. CO_2 capture from simulated flue gas is exemplified by PAF-18-OH and PAF-18-OLi. In the case of PAF-18-OLi, high CO_2/N_2 selectivity, up to 129 under ambient temperature and pressure is obtained, the value of which is almost four times higher than that of PAF-18-OH at the same condition. Notably, PAF-18-OLi material also exhibits high stability. The development of high-performance porous organic frameworks with remarkably high CO_2/N_2 selectivity, excellent sorption

capacity of CO_2 and H_2, and high stability would pave its significant way in carbon dioxide capture and sequestration, and hydrogen storage.

Acknowledgments

We are grateful for the financial support of National Basic Research Program of China (973 Program, grant nos. 2012CB821700), Major International (Regional) Joint Research Project of NSFC (grant nos.21120102034) and NSFC (grant nos. 20831002).

Notes and references

[a] *State Key Laboratory of Inorganic Synthesis & Preparative Chemistry, Jilin University, Changchun, 130012, China.*
Fax: (+86)431-8516-8331
E-mail: zhugs@jlu.edu.cn
[b] *Ian Wark Research Institute University of South Australia Mawson Lakes Campus Adelaide, SA 5095, Australia*
[c] *Queensland Micro- and Nanotechnology Centre, Griffith University, Queensland, 4111, Australia.*

† Electronic Supplementary Information (ESI) available: [This material includes: XRD, SEM, IR, TG, XPS figures; CO_2 and H_2 adsorption isotherms of PAF-18-OLi with different Li contents as well as details on the calculations of Q_{st} and selectivity from ideal adsorption solution theory (IAST)]. See DOI: 10.1039/b000000x/

1 IPCC, 2007: Summary for Policymakers. In: Climate Change 2007: The Physical Science Basis, Cambridge University Press, Cambridge, UK, 2007.

2 a) S. Keskin, T. M. van Heest, D. S. Sholl, *ChemSusChem.*, 2010, **3**, 879; b) S. Chu, *Science*, 2009, **325**, 1599; c) R. S. Haszeldine, *Science*, 2009, *325*, 1647; d) J. Sculley, D. Yuan, H. C. Zhou, *Energy. Environ. Sci.*, 2011, **4**, 2721.

3 a) Y. S. Bae, R. Q. Snurr, *Angew. Chem. Int. Ed.*, 2011, **50**, 11586; b) D. M. DAlessandro, B. Smit, J. R. Long, *Angew. Chem*., 2010, **122**, 6194; *Angew. Chem. Int. Ed.*, 2010, **49**, 6058.

4 a) L. Schlapbach, A. Züttel, *Nature*, 2001, **414**, 353; b) U. Eberle, M. Felderhoff, F. Schüth, *Angew. Chem. Int. Ed.*, 2009, **48**, 6608; c) V. V. Struzhkin, B. Militzer, W. L. Mao, H. Mao, R. J. Hemley, *Chem. Rev*., 2007, **107**, 4133.

5 a) X. Peng, W. C. Wang, R. S. Xue, Z. M. Shen, *AIChE J.*, 2006, **52**, 994; b) M. B. Kim, Y. S. Bae, D. K. Choi, C. H. Lee, *Ind. Eng. Chem. Res.*, 2006, **45**, 5050; c) V. Goetz, O. Pupier, A. Guillot, *Adsorption*, 2006, **12**, 55.

6 a) S. Cavenati, C. A. Grande, A. E. Rodrigues, *J. Chem. Eng. Data.*, 2004, **49**, 1095; b) P. Y. Li, F. H. Tezel, *Microporous Mesoporous Mater*., 2007, **98**, 94; c) J. M. Leyssale, G. K. Papadopoulos, D. N. Theodorou, *J. Phys. Chem. B*, 2006, **110**, 22742; d) R. Babarao, Z. Q. Hu, J. W. Jiang, S. Chempath, S. I. Sandler, *Langmuir*, 2007, **23**, 659.

7 a) M. Eddaoudi, J. Kim, N. Rosi, D. Vodak, J. Wachter, M. O'Keeffe, O. M. Yaghi, *Science*, 2002, **295**, 469; b) G. Férey, C. M. Draznieks, C. Serre, F. Millange, J. Dutour, S. Surblé, I. Margiolaki, *Science*, 2005, **309**, 2040; c) J. S. Seo, D. Whang, H. Lee, S. I. Jun, J. Oh, Y. J. Jeon, K. Kim, *Nature*, 2000, **404**, 982; d) D. M. D'Alessandro, B. Smit, J. R. Long, *Angew. Chem. Int. Ed.*, 2010, **49**, 2; e) B. Q. Ma, K. L. Mulfort, J. T. Hupp, *Inorg. Chem.*, 2005, **44**, 4912; f) S. Kitagawa, R. Kitaura, S. Noro, *Angew. Chem. Int. Ed.*, 2004, **43**, 2334; g) B. Zheng, J. Bai, J. Duan, L. Wojtas, M. J. Zaworotko, *J. Am. Chem. Soc*., 2011, **133**, 748; h) R. Luebke, J. F. Eubank, A. J. Cairns, Y. Belmabkhout, L. Wojtas, M. Eddaoudi, *Chem. Commun.*, 2012, **48**, 1455; i) B. L. Chen, S. Q. Ma, F. Zapata, F. R. Fronczek, E. B. Lobkovsky, H. C. Zhou. *Inorg. Chem.*, 2007, **46**, 1233; j) B. L. Chen, X. B. Zhao, A. Putkham, K. Hong, E. B. Lobkovsky, E. J. Hurtado, A. J. Fletcher, K. M. Thomas. *J. Am. Chem. Soc.*, 2008, **130**, 6411.

8 a) J. X. Jiang, F. Su, A. Trewin, C. D. Wood, N. L. Campbell, H. Niu, C. Dickinson, A. Y. Ganin, M. J. Rosseinsky, Y. Z. Khimyak, A. I. Cooper, *Angew. Chem. Int. Ed.*, 2007, **46**, 8574; b) M. P. Tsyurupa, V. A. Davankov, *React. Funct. Polym*., 2002, **53**, 193.

9 a) N. B. McKeown, P. M. Budd, K. J. Msayib, B. S. Ghanem, H. J. Kingston, C. E. Tattershall, S. Makhseed, K. J. Reynolds, D. Fritsch, *Chem.–Eur. J*., 2005, **11**, 2610; b) N. B. McKeown, P. M. Budd, *Chem. Soc. Rev.*, 2006, **35**, 675.

10 L. Chen, Y. Honsho, S. Seki, D. Jiang, *J. Am. Chem. Soc*., 2010, **132**, 6742.

11 a) T. Ben, H. Ren, S. Q. Ma, D. P. Cao, J. H. Lan, X. F. Jing, W. C. Wang, J. Xu, F. Deng, J. M. Simmons, S. L. Qiu, G. S. Zhu, *Angew. Chem. Int. Ed.*, 2009, **48**, 9457; b) H. Ren, T. Ben, F. Sun, M. Guo, H. Ma, K. Cai, S. L. Qiu, G. S Zhu，*J. Mater. Chem.*, 2011, **21**, 10348; c) H. Ren, T. Ben, E. S. Wang, X. F. Jing, M. Xue, B. B. Liu, Y. Cui, S. L. Qiu, G. S. Zhu, *Chem. Commun.*, 2010, **46**, 291; d) W. Lu, D. Yuan, D. Zhao, C. I. Schilling, O. Plietzsch, T. Muller, S. Bräse, J. Guenther, J. Blümel, R. Krishna, Z. Li, H. C. Zhou, *Chem. Mater*., 2010, **22**, 5964; e) W. Wang, H. Ren, F. Sun, K. Cai, H. P. Ma, J. Du, H. Zhao, G. S. Zhu, *Dalton Trans*., 2012, **41**, 3933; f) X. Jing, F. Sun, H. Ren, Y. Tian, M. Guo, L. Li, G. S. Zhu, *Microporous Mesoporous Mater*., 2013, **165**, 92; g) Y. Yuan, F. Sun, H. Ren, X. Jing, W. Wang, H. Ma, H. Zhao, G. S. Zhu, *J. Mater. Chem*., 2011, **21**, 13498.

12 H. Furukawa, O. M. Yaghi, *J. Am. Chem. Soc.*, 2009, **131**, 8875; b) A. P. Cote, A. I. Benin, N. W. Ockwig, M. O'Keeffe, A. J. Matzger, O. M. Yaghi, *Science*, 2005, **310**, 1166; c) H. M. Kaderi, J. R. Hunt, J. L. Mendoza, A. P. Cote, R. E. Taylor, M. O'Keeffe, O. M. Yaghi, *Science*, 2007, **316**, 268.

13 P. Kuhn, M. Antonietti, A. Thomas, *Angew. Chem. Int. Ed.*, 2008, **47**, 3450.

14 a) E. R. Thomas, T. J. Karl, S. Li, J. Puru, M. E. Hani, *J. Mater. Chem.*, 2011, **21**, 10629; b) Y. H. Jin, B. A.Voss, R. D.Noble, W. Zhang, *Angew. Chem. Int. Ed.*, 2010, **49**, 6348; c) R. Dawson, E. Stöckel, J. R. Holst, D. J. Adams, A. I. Cooper, *Energy Environ. Sci.*, 2011, **4**, 4239.

15 A. L. Chaffee, G. P. Knowles, Z. Liang, J. Zhany, P. Xiao, P. A. Webley, *Int. J. Greenhouse Gas Control*, 2007, **1**, 11.

16 D. Aaron, C. Tsouris, *Sep. Sci. Technol.*, 2005, **40**, 321.

17 a) Y. S. Bae, A. M. Spokoyny, O. K. Farha, R. Q. Snurr, J. T. Hupp, C. A. Mirkin, *Chem. Commun.*, 2010, **46**, 3478; b) Z. Q. Wang, S. M. Cohen, *Chem. Soc. Rev.*, 2009, **38**, 1315; c) R. Dawson, D. J. Adams, A. I. Cooper, *Chem. Sci*., 2011, **2**, 1173; d) D. Himsl, D. Wallacher, M. Hartmann, *Angew. Chem.*, 2009, **121**, 4710; *Angew.Chem. Int. Ed*., 2009, **48**, 4639.

18 a) Y. J. Choi, J. W. Lee, J. H. Choi, J. K. Kang, *Appl. Phys. Lett.*, 2008. **92**, 173102; b) J. Lan, D. Cao, W. Wang, B. Smit, *ACS Nano*, 2010, **4**, 4225; c) A. Mavrandonakis, E. Tylianakis, A. K. Stubos, G. E. Froudakis, *J. Phys. Chem. C*, 2008, **112**, 7290; d) A. Blomqvist, C. M. Araujo, P. Srepusharawoot, R. Ahuja, *Proc. Natl. Acad. Sci.*, 2007. **104**, 20173.

19 a) K. L. Mulfort, O. K. Farha, C. L. Stern, A. A. Sarjeant, J. T. Hupp, *J. Am.Chem. Soc*., 2009, **131**, 3866; b) Z. Xiang, Z. Hu, D. Cao, W. Yang, J. Lu, B. Han, W. Wang, *Angew. Chem. Int. Ed.*, 2011, **50**, 491; c) A. Li, R. Lu, Y. Wang, X. Wang, K. Han, W. Deng, *Angew. Chem. Int. Ed.*, 2010, **49**, 3330; d) K. L. Mulfort, J. T. Hupp, *J. Am.Chem. Soc.*, 2007, **129**, 9604; e) D. Himsl, D. Wallacher,M. Hartmann, *Angew. Chem. Int. Ed.*, 2009, **48**, 4639; f) S. Yang, X. Lin, A. J. Blake, K. M. Thomas, P. Hubberstey, N. R. Champness, M. Schröder, *Chem. Commun.*, 2008, 6108; g) K. L. Mulfort, T. M. Wilson, M. R. Wasielewski, J. T. Hupp, *Langmuir*, 2009, **25**, 503; h) F. Nouar, J. Eckert, J. F. Eubank, P. Forster, M. Eddaoudi, *J. Am. Chem. Soc.*, 2009, **131**, 2864.

20 a) W. Lu, D. Yuan, D. Zhao, I. S. Christine, O. Plietzsch, T. Muller, S. Bräse, J. Guenther, J Blümel, R Krishna, Z. Li, H. C. Zhou, *Chem. Mater*., 2010, **22**, 5964; b) E. Kiehlmann, R. W. Lauener, *Can. J. Chem.*, 1989, **67**, 335.

21 The palladium-catalyzed Sonogashira-Hagihara cross-coupling reaction is also known for the synthesis of conjugated microporous polymers (CMPs) reported by the group of Andrew I. Cooper. See: a) R. Dawson, A. I. Cooper, D. J. Adams, *Prog. Polym. Sci.*, 2012, **37**, 530; b) J. X. Jiang, F. Su, A. Trewin, C. D. Wood, H. Niu, J. T. A.

Jones, Y. Z. Khimyak, A. I. Cooper. *J. Am. Chem. Soc.*, 2008, **130**, 7710; c) J. X. Jiang, A. Trewin, F. Su, C. D. Wood, H. Niu, J. T. A. Jones, Y. Z. Khimyak, A. I. Cooper, *Macromolecules*, 2009, **42**, 2658; d) R. Dawson, A. Laybourn, R. Clowes, Y. Z. Khimyak, D. J. Adams, A. I. Cooper, *Macromolecules*, 2009, **42**, 8809.

22 M. Inagaki, O. Tanaike, *Synth. Met.*, 1995, **73**, 77.

23 J. P. Contour, A. Salesse, M. Froment, M. Garreau, J. Thevenin, D. Warin, *J. Microsc. Spectrosc. Electron.*, 1979, **4**, 483.

24 R. Dawson, A. Laybourn, Y. Z. Khimyak, D. J. Adams, A. I. Cooper, *Macromolecules*, 2010, **43**, 8524.

25 a) W. Lu, D. Yuan, J. Sculley, D. Zhao, R. Krishna, H. C. Zhou, *J. Am. Chem. Soc.*, 2011, **133**, 18126; b) E. D. Bloch, D. Britt, C. Lee, C. J. Doonan, F. J. Uribe-Romo, H. Furukawa, J. R. Long, O. M. Yaghi, *J. Am. Chem. Soc.*, 2010, **132**, 14382.

26 a) R. C. Lochan, M. Head-Gordon, *Phys. Chem. Chem. Phys.*, 2006, *8*, 1357; b) S. K. Bhatia, A. L. Myers, *Langmuir*, 2006, **22**, 1688.

27 Q. Xu, D. H. Liu, Q. Y. Yang, C. L. Zhong, J. G. Mi, *J. Mater.Chem.*, 2010, **20**, 706.

28 a) Y. S. Bae, A. M. Spokoyny, O. K. Farha, R. Q. Snurr, J. T. Hupp, C. A. Mirkin, *Chem. Commun.*, 2010, **46**, 3478; b) Y. J. Choi, J. W. Lee, J. H. Choi, J. K. Kang, *Appl. Phys. Lett.*, 2008. **92**, 173102 ; c) R. Dawson, D. J. Adams, A. I. Cooper, *Chem. Sci.*, 2011, **2,** 1173; d) A. Mavrandonakis, E. Tylianakis, A. K. Stubos, G. E. Froudakis, *J. Phys. Chem. C*, 2008, **112**, 7290.